

COBEM-2017-0995

THE INFLUENCE OF HEAT TREATMENTS ON Ni-Ti SPRINGS HYSTERESIS LOOP

H. S. Oliveira
S. A. Bandeira
A. S. de Paula

University of Brasilia - Department of Mechanical Engineering - Campus Universitario Darcy Ribeiro
hso.smas@gmail.com, sbandeira@outlook.com, alinedepaula@unb.br

Abstract. *The influence of heat treatments on shape memory alloys is investigated with respect to changes in hysteresis loop of NiTi springs. Some aging temperatures are evaluated regarding the precipitation and growth of Ti_3Ni_4 . The influence of these precipitates is then evaluated in terms of the area of hysteresis loop, distribution of precipitates and transformation temperatures.*

Keywords: *shape memory alloy, hysteresis loop, Ti_3Ni_4*

1. INTRODUCTION

Shape memory alloys are materials that present characteristics of great interest in various technological sectors. The current literature presents several applications in diverse areas such as civil construction, dental materials, electronic equipment, and aerospace devices (Kumar and Lagoudas, 2008; Otsuka and Ren, 2005; Duerig *et al.*, 1990; Mahmud, 2009; Liu *et al.*, 1997). Some of these applications enhance the performance of existing technologies, and others significantly simplify design difficulties, creating new opportunities and functionalities that would be impossible without those materials.

The phenomena related to pseudo-elasticity and shape memory effect are the key factors that have attracted much attention to this material (Duerig *et al.*, 1990). The ability to respond to external stimuli in a differentiated way makes them considered as Intelligent and Functional Materials, and can be applied in several areas. Among the several existing shape memory materials, Ni-Ti binary alloy has been one of the most extensively studied. It exhibits an intense nonlinear response related to shape memory effect and pseudo-elasticity under certain conditions. It is also strongly affected by metallurgical conditions and its chemical composition (Mahmud, 2009). Therefore, various thermal and mechanical treatments have been used as effective tools to manipulate its behavior (Otsuka and Ren, 2005; Liu *et al.*, 1997; Lin and Wu, 1993).

With respect to the ability to produce precipitates from heat treatments, Ni-Ti alloys are divided into two subclasses: near-equiatomic (nickel concentration equal or less than 50.5% Ni); and Ni-rich (nickel concentration greater than 50.5% Ni). Corresponding to these two subclasses, there are two main types of treatments: cold work with subsequent annealing; and aging, respectively. Although there are many studies that address the effect of heat treatment on pseudoelastic behavior and shape memory effect (Duerig *et al.*, 1990; Lin and Wu, 1993; Okamoto *et al.*, 1988; Liu and McCormick, 1994; Nishida *et al.*, 1986), few papers focus on the influence of heat treatment on the area and energy dissipation of the hysteresis loop of NiTi alloys.

This study evaluates quantitatively how aging at different temperatures and times can change the hysteresis loop in pseudoelastic regime. Understanding the hysteresis loop shape is vital for applications in engineering (Frick *et al.*, 2005). It is necessary for the development of devices that aim not only energy dissipation or shape memory effect but also at dynamic applications such as adaptive dynamic absorbers of vibrations. The stiffness in these equipment is due to the shape memory alloy and its hysteresis loop is fundamental for the design of nonlinear dynamic systems.

2. EXPERIMENTAL PROCEDURES

The experiment is conducted through Ni(50,7%)-Ti traction springs from Kellogg's Research Labs. Their geometrical characteristics are presented in Tab. 1. Initially, all the springs are submitted to a solubilization treatment at 700°C for 60 min without inert atmosphere and subsequent tempering in water at room temperature (around 27°C). These solubilized springs are submitted to aging treatment at 400°C for different periods of time, seeking the precipitation of Ti_3Ni_4

according to Tab. 2. Note that spring S1 is only submitted to solubilization.

Table 1. Geometrical Characteristics of the springs

Wire Diameter	1.25 mm
Mandrel Size	9.7 mm
Pitch	1.22 mm
Lentgh	12.7 mm

After the heat treatments, the direct and inverse transformations temperatures are analyzed by means of a Differential Scanning Calorimetry (DSC) through a DSC-8000 from Perkin Elmer. A sweep from -70°C to 100°C at $20^{\circ}\text{C}/\text{min}$ is carried out to identify the direct transformations temperatures, while a sweep from 100°C to -70°C at $-20^{\circ}\text{C}/\text{min}$ is carried out to identify the temperatures of the inverse transformations.

Table 2. Heat Treatments

Sample	Aging Time
S1	-
S2	30min
S3	60min
S4	90min
S5	120min

After the transformations temperatures are identified, the hysteresis loop is stabilized through 200 loading-unloading cyclical test carried out at constant temperature that assures the material is in pseudoelastic regime.

3. RESULTS

Results from DSC analysis and stabilized hysteresis loops are exposed below.

3.1 Solubilization at 700°C

Figure 1 shows the transformation temperatures after the solubilization at 700°C with subsequent tempering. The presence of only one peak in the direct (cooling) and inverse transformation (heating) is the main characteristic observed. According to Fan *et al.* (2004) and Frick *et al.* (2005), heat treatments above the recrystallization temperature result in a solubilization of the exceeding nickel. Therefore, there will not be precipitates or defects, such as dislocations. Fan *et al.* (2004) and Khalil-Allafi *et al.* (2002) point out that the two peaks in the direct and inverse transformations are related to $B_2 \rightarrow B'_{19}$ and $B'_{19} \rightarrow B_2$ transitions respectively. Nevertheless, it is important to consider the presence of oxidation points Ti_4NiO_2 in the microstructure due the lack of inert atmosphere during the heat treatments. Figure 2(a) presents a sketch of the microstructure obtained from the solubilization treatment. It is observable the presence of oxidation points but - due to the solubilization treatment - there is no precipitates or dislocations in the microstructure.

3.2 Aging

After the solubilization at 700°C for 60min, aging at 400°C was carried out at different periods of time much likely what was developed in Fan *et al.* (2004) , Frick *et al.* (2005), Khalil-Allafi *et al.* (2002), Khalil-Allafi *et al.* (2004), Zheng *et al.* (2008) and Jiang *et al.* (2009).

3.2.1 Aging at 400°C for 30min

At 400°C for 30min, it can be observed the occurrence of three peaks (indicated by arrows in Figure 1(b)). According to the theory proposed by Fan *et al.* (2004), it is a consequence of a inhomogeneous distribution of Ti_3Ni_4 precipitates in grain boundary, that is, the concentration of Ti_3Ni_4 is higher at the boundary than in the interior of the grains.

Grain boundaries reduces the driving force for Ti_3Ni_4 nucleation and, as a consequence, it first nucleates at the grain boundaries. The formation of Ti_3Ni_4 reduces the concentration of nickel at its surroundings, favoring the transition $B_2 \rightarrow R$ at the grain boundary. The precipitates also imposes a resistance to the transition $B_2 \rightarrow B'_{19}$ at the grain boundary. Therefore, the first peak in Figure 1(b) is understood as $B_2 \rightarrow R$.

The lack of inert atmosphere is a factor the must also be considered in the analysis. Thereby, it is natural to assume that there are Ti_4NiO_2 oxidation points inside the grains and at its boundary because they also favors the precipitation of Ti_3Ni_4 . Therefore, the first peak must also represent the transition $B_2 \rightarrow R$ around the oxidation points (Mahmud,

2009).

The second peak in the direct transformation (Figure 1-b) occurs at a temperature close to the temperature of transition $B_2 \rightarrow B'_{19}$ verified in the solubilization (Figure 1-a). This peak is related to the one-stage transition $B_2 \rightarrow B'_{19}$ in the interior of grains where there is no influence of oxidation points and Ti_3Ni_4 . However, still have the same concentration of Ni observed in the solubilization treatment.

The third peak represents the transition $R \rightarrow B'_{19}$. The reason it occurs at very low temperatures when compared to $B_2 \rightarrow B'_{19}$. This behavior is associated to a higher driving force needed which is only reached through high temperature variations (Fan *et al.*, 2004).

Figure 2(b) exhibits the microstructure that can be expected when dealing with this sort of heat treatment (Fan *et al.*, 2004; Khalil-Allafi *et al.*, 2002, 2004). There are precipitates around the grain boundary as well as around the oxidation points with some areas free of oxidation points and precipitates.

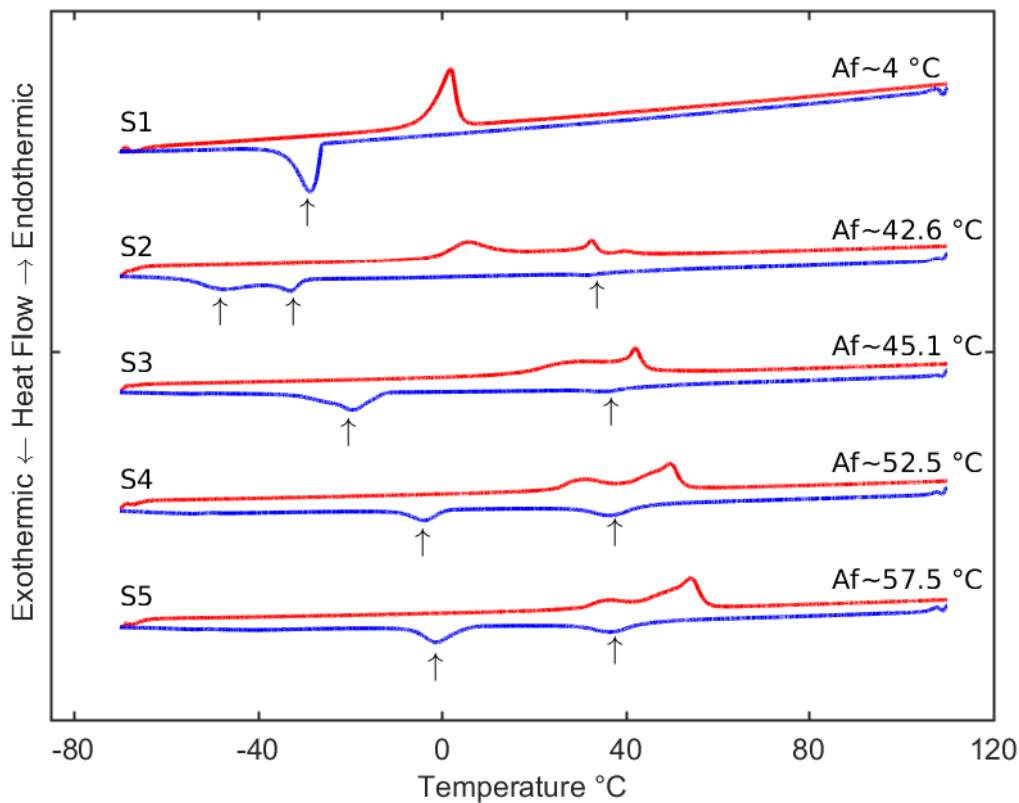


Figure 1. Characteristic temperatures and peaks obtained through DSC.

3.2.2 Aging at 400°C for higher periods of time

When the material is exposed to the aging temperature at higher periods of times, the precipitates keep nucleating and growing, either by the continuous absorption of the supersaturated nickel present in B_2 phase or by the absorption of smaller precipitates by larger ones (Fan *et al.*, 2004). Thereafter, both concentration of Ni at the grain boundary and the interior are reduced with aging time.

By the time the precipitates grow and reduce the concentration of Ni at the grain interior and at the boundary, Ti_4NiO_2 keeps being formed. These oxidation points reduce the concentration of Ti resulting in an increase of Ni concentration, which influences in the nucleation and growth of Ti_3Ni_4 around them (Michutta *et al.*, 2006; Fan *et al.*, 2004). Therefore, depending on the concentration and distribution of oxidation points in the microstructure, a higher homogeneity in Ti_3Ni_4 is expected, since there is no significant difference in the nucleation rate between the grain interior and the grain boundary. This fact results in only two peaks of transformation Figure 1 (b,c,d,e) (Fan *et al.*, 2004).

The first peak is related to the transition $B_2 \rightarrow R$. At this point the transformation temperature depends mainly on concentration of Ni in B_2 and is less influenced by the size of the particles. Thus the temperature of the transition $B_2 \rightarrow R$ is not significantly shifted even after a prolonged period of time at 400°C Figure 1(b,c,d,e) (Fan *et al.*, 2004).

The second peak is related to the transition $R \rightarrow B'_{19}$. It is noticeable that the transition temperature shifts along with

aging time. It is a consequence of the precipitation size growth, which reduces the resistance to the formation of B'_{19} , resulting in a lower variation of temperature (Fan 2004).

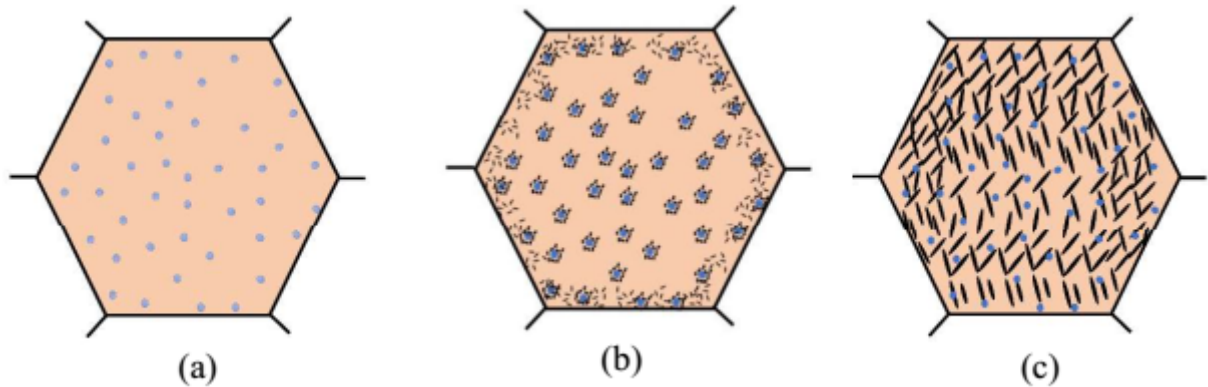


Figure 2. Probable microstructure obtained from the treatments and defined by Fan et al (2004).

3.3 Evaluation of the hysteresis loop and dissipated energy per cycle

After heat treatments and the analysis through DSC, the influence of the microstructure in the hysteresis loop is analyzed. However, it is necessary to stabilize the hysteresis loop at constant temperatures above A_f (austenite final temperature) (Kumar and Lagoudas, 2008). The stabilization is performed through an equipment designed specifically for this purpose at the Laboratory of Vibration at the University of Brasilia (Figure 3).



Figure 3. Equipment specifically designed for stabilizations of Niti springs at constant temperatures.

The equipment is fully automated through the open-source single-board microcontroller Arduino Mega. The device automates the load and unload by means of a loadcell and a laser distance sensor.

The stabilization is carried out by application of 200 loading-unloading cycles of $46.5N$. This process can induce changes in microstructure which can result in residual deformations macroscopically observable (Kumar and Lagoudas,

2008).

After stabilization, results are divided in two parts. At first, hysteresis loops are presented considering prescribed loading and then prescribed dislocation if of concern.

3.3.1 Prescribed Loading

Figure 4 presents the hysteresis loop obtained after the stabilization. The testing temperature were always above A_f , assuring the pseudoelastic regime. In Figure 4(a), spring S1 presents the smallest area of hysteresis loop, that is, the lowest dissipation energy per hysteresis cycle. It is associated to the microstructure presented in Figure 5(a), where there is no precipitates Ti_3Ni_4 .

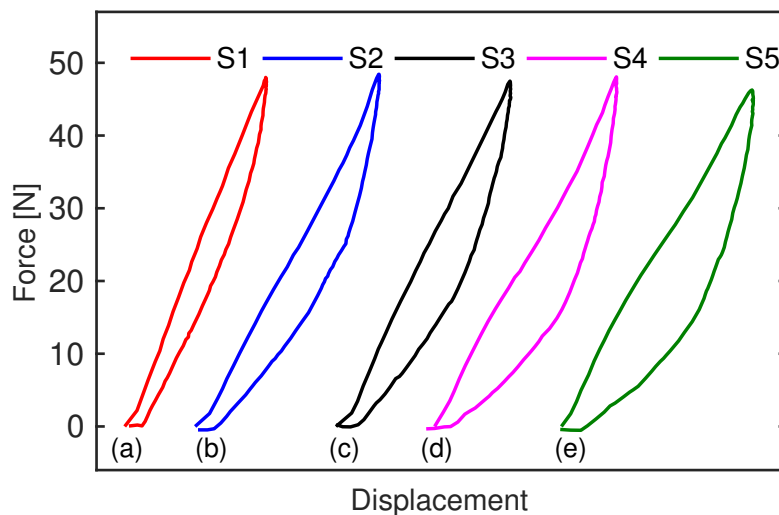


Figure 4. Hysteresis loop obtained after a 46.5N cyclic loading-unloading: (a) at 30°C; (b) at 45°C; (c) at 55°C; (d) at 55°C; (e) at 58°C.

Figure 4(b) is a result of the microstructure presented in Figure 2(b), which presents a higher hysteresis loop area when compared to the spring S1. The presence of precipitates results in a higher dissipation per cycle. However, when the aging time increases, it is observable that energy dissipation per cycle increases (Figure 4-c,d,e). These results might be a consequence of the reduction of Ni concentration in B_2 due to the nucleation and growth of precipitates.

Figure 5 presents the hysteresis area for each heat treatment performed. It is noticeable that the nucleation and growth of Ti_3Ni_4 along with the reduction of Ni in B_2 results in an increase of the energy dissipated per cycle.

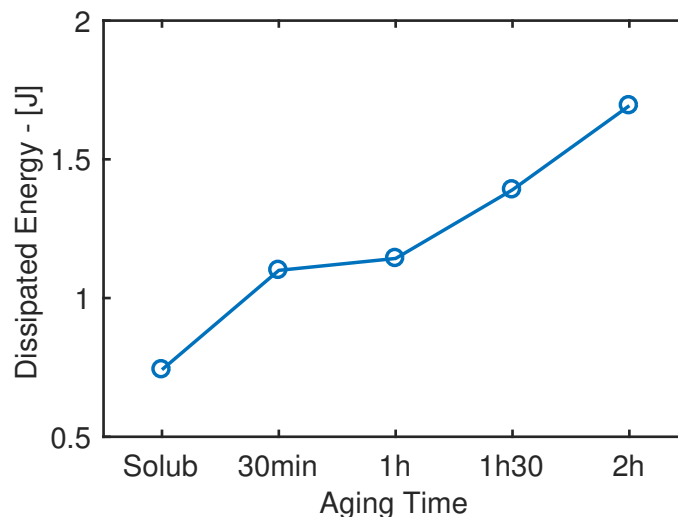


Figure 5. Energy dissipation per cycle for prescribed loading

3.3.2 Prescribed Displacement

In the prescribed dislocation analysis, the required force to reach the prescribed value (20cm) is higher for the spring S1 (Figure 6-a) (Jiang *et al.*, 2009). Again, the hysteresis loop for spring S1 is significantly smaller than the other cases.

For spring S2 ((Figure 6-b), the required force is necessary to reach the same prescribed displacement is the lowest. This behavior is associated to the presence of Ti_3Ni_4 in the boundary grain, around the oxidation points and the area which is not influenced.

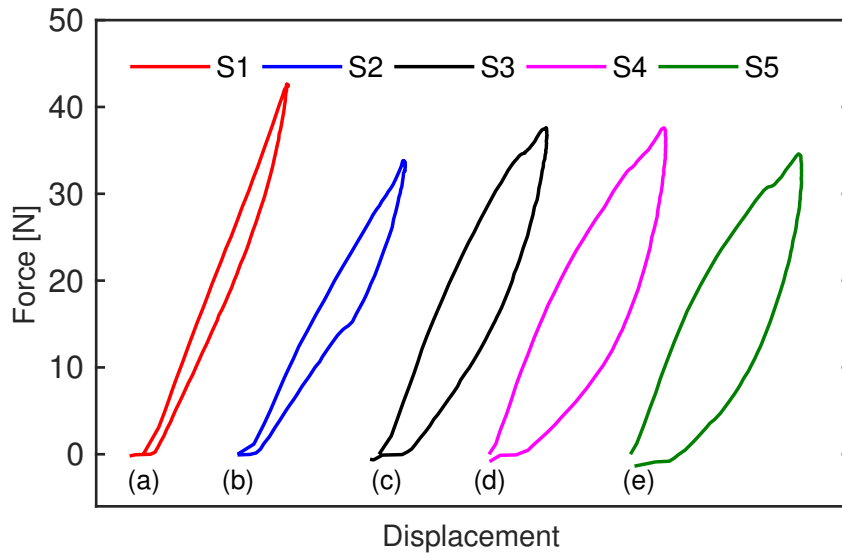


Figure 6. Hysteresis loop obtained after a cyclic constant displacement of 20 cm: (a) at 30°C; (b) at 45°C; (c) at 55°C; (d) at 55°C; (e) at 58°C.

The hysteresis loop area increases for each case in the prescribed displacement analysis (Figure 6-c,d,e). Nevertheless the force required do not significantly change. These behavior are a consequence of the resulting microstructure, much likely the prescribed loading analysis. The energy dissipated per cycle can be evaluated by means of Figure 7, which presents the same tendency presented in the prescribed loading analysis.

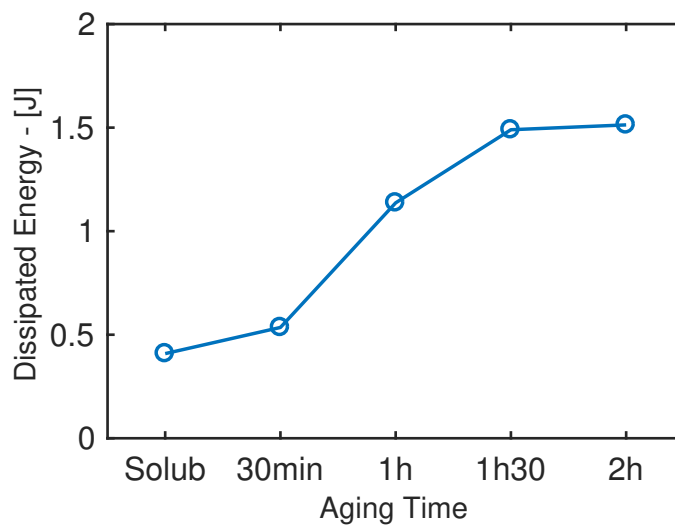


Figure 7. Energy dissipation per cycle for prescribed displacement

4. CONCLUSION

This paper dealt with the influence of heat treatments on *NiTi* springs hysteresis loop. Results show there is noticeable correlation between the presence of precipitates Ti_3Ni_4 and dislocations with the hysteresis loop and energy dissipated

per cycle in a Ni(50,7%)-Ti.

The case where the spring was only submitted to solubilization, that is, lack of precipitates and dislocations presented only two peaks of transformations and low dissipation of energy per cycle after the hysteresis loop stabilization.

The other cases, where the springs were submitted to different aging times after the solubilization, the transformation temperatures increased significantly along with the presence of a more peaks of transformation. The energy dissipated per cycle increased with the aging time.

This work is a step toward a more dense study about applications of SMAs. So far it can be concluded that for applications where high dissipation of mechanical energy is desired, springs with Ti_3Ni_4 is a reasonable choice.

5. ACKNOWLEDGEMENTS

The authors would like to acknowledge the support of CNPq.

6. REFERENCES

- Duerig, T.W., Zadno, G.R. and Melton, K.N., 1990. "Ni-Ti Based Shape Memory Alloys". In T.W. Duerig, ed., *Eng. Asp. Shape Mem. Alloy.*, Elsevier {BV}, pp. 21–35. doi:10.1016/b978-0-7506-1009-4.50006-8.
- Fan, G., Chen, W., Yang, S., Zhu, J., Ren, X. and Otsuka, K., 2004. "Origin of abnormal multi-stage martensitic transformation behavior in aged Ni-rich TiNi shape memory alloys". *Acta Mater.*, Vol. 52, No. 14, pp. 4351–4362. ISSN 13596454. doi:10.1016/j.actamat.2004.06.002. URL <http://linkinghub.elsevier.com/retrieve/pii/S1359645404003271>.
- Frick, C.P., Ortega, A.M., Tyber, J., Maksound, A., Maier, H.J., Liu, Y. and Gall, K., 2005. "Thermal processing of polycrystalline NiTi shape memory alloys". *Mater. Sci. Eng. A*, Vol. 405, No. 1-2, pp. 34–49. ISSN 09215093. doi:10.1016/j.msea.2005.05.102. URL <http://linkinghub.elsevier.com/retrieve/pii/S0921509305005563>.
- Jiang, F., Liu, Y., Yang, H., Li, L. and Zheng, Y.f., 2009. "Effect of ageing treatment on the deformation behaviour of Ti-50.9 at.%Ni". *Acta Mater.*, Vol. 57, No. 16, pp. 4773–4781. ISSN 13596454. doi:10.1016/j.actamat.2009.06.059. URL <http://linkinghub.elsevier.com/retrieve/pii/S1359645409003930>.
- Khalil-Allafi, J., Dlouhý, A. and Eggeler, G., 2002. "Ni₄Ti₃-precipitation during aging of NiTi shape memory alloys and its influence on martensitic phase transformations". *Acta Mater.*, Vol. 50, No. 17, pp. 4255–4274. ISSN 13596454. doi:10.1016/S1359-6454(02)00257-4. URL <http://linkinghub.elsevier.com/retrieve/pii/S1359645402002574>.
- Khalil-Allafi, J., Eggeler, G., Dlouhý, A., Schmahl, W.W. and Somsen, C., 2004. "On the influence of heterogeneous precipitation on martensitic transformations in a Ni-rich NiTi shape memory alloy". *Mater. Sci. Eng. A*, Vol. 378, No. 1-2, pp. 148–151. ISSN 09215093. doi:https://doi.org/10.1016/j.msea.2003.10.335. URL <http://linkinghub.elsevier.com/retrieve/pii/S092150930301534X>.
- Kumar, P.K. and Lagoudas, D.C., 2008. "Introduction to Shape Memory Alloys". Springer US, 1, chapter 1, pp. 1–43. 1st edition. URL <http://gen.lib.rus.ec/book/index.php?md5=ABC45914E87E43E9ACB13D99FFFD4EC1>.
- Lin, H.C. and Wu, S.K., 1993. "Determination of heat of transformation in a cold-rolled martensitic TiNi alloy". *Metall. Trans. A*, Vol. 24, No. 2, pp. 293–299. ISSN 0360-2133. doi:10.1007/BF02657316. URL <http://link.springer.com/10.1007/BF02657316>.
- Liu, Y., Chen, X. and McCormick, P.G., 1997. "No Title". *J. Mater. Sci.*, Vol. 32, No. 22, pp. 5979–5984. ISSN 00222461. doi:10.1023/A:1018615127911. URL <http://link.springer.com/article/10.1023/A:1018615127911>.
- Liu, Y. and McCormick, P.G., 1994. "Thermodynamic analysis of the martensitic transformation in NiTi-I. Effect of heat treatment on transformation behaviour". *Acta Metall. Mater.*, Vol. 42, No. 7, pp. 2401–2406. ISSN 09567151. doi:10.1016/0956-7151(94)90318-2. URL <http://linkinghub.elsevier.com/retrieve/pii/0956715194903182>.
- Mahmud, A.S., 2009. *Thermomechanical Treatment of Ni-Ti Shape Memory Alloy*. Phd thesis, School of Mechanical Engineering - The University of Western Australia.
- Michutta, J., Somsen, C., Yawny, A., Dlouhý, A. and Eggeler, G., 2006. "Elementary martensitic transformation processes in Ni-rich NiTi single crystals with Ni₄Ti₃ precipitates". *Acta Mater.*, Vol. 54, No. 13, pp. 3525–3542. ISSN 13596454. doi:10.1016/j.actamat.2006.03.036. URL <http://linkinghub.elsevier.com/retrieve/pii/S1359645406002345>.
- Nishida, M., Wayman, C.M. and Honma, T., 1986. "Precipitation processes in near-equiatom NiTi shape memory alloys". *Metall. Trans. A*, Vol. 17, No. 9, pp. 1505–1515. doi:10.1007/bf02650086.
- Okamoto, Y., Hamanaka, H., Miura, F., Tamura, H. and Horikawa, H., 1988. "Reversible changes in yield stress and transformation temperature of a NiTi alloy by alternate heat treatments". *Scr. Metall.*, Vol. 22, No. 4, pp. 517–520. doi:10.1016/0036-9748(88)90016-6.
- Otsuka, K. and Ren, X., 2005. "Physical metallurgy of Ti-Ni-based shape memory alloys". *Prog. Mater. Sci.*, Vol. 50,

No. 5, pp. 511–678. doi:10.1016/j.pmatsci.2004.10.001.

Zheng, Y., Jiang, F., Li, L., Yang, H. and Liu, Y., 2008. “Effect of ageing treatment on the transformation behaviour of Ti50.9at%Ni alloy”. *Acta Mater.*, Vol. 56, No. 4, pp. 736–745. ISSN 13596454. doi:10.1016/j.actamat.2007.10.020. URL <http://linkinghub.elsevier.com/retrieve/pii/S1359645407007112>.

7. RESPONSIBILITY NOTICE

The authors are the only responsible for the material included in this paper.